Bioelectric impact of pathological angiogenesis on vascular function

Donald G. Puro[a,b,1], Ryohsuke Kohmoto[a], Yasushi Fujita[a], Thomas W. Gardner[a,b], and Dolly A. Padovani-Claudio[a]

[a]Department of Ophthalmology and Visual Sciences, University of Michigan, Ann Arbor, MI 48105; and [b]Department of Molecular and Integrative Physiology, University of Michigan, Ann Arbor, MI 48105

Edited by John E. Dowling, Harvard University, Cambridge, MA, and approved June 30, 2016 (received for review March 22, 2016)

Pathological angiogenesis, as seen in many inflammatory, immune, malignant, and ischemic disorders, remains an immense health burden despite new molecular therapies. It is likely that further therapeutic progress requires a better understanding of neovascular pathophysiology. Surprisingly, even though transmembrane voltage is well known to regulate vascular function, no previous bioelectric analysis of pathological angiogenesis has been reported. Using the perforated-patch technique to measure vascular voltages in human retinal neovascular specimens and rodent models of retinal neovascularization, we discovered that pathological neovessels generate extraordinarily high voltage. Electrophysiological experiments demonstrated that voltage from aberrantly located preretinal neovascular complexes is transmitted into the intraretinal vascular network. With extensive neovascularization, this voltage input is substantial and boosts the membrane potential of intraretinal blood vessels to a suprahyperpolarized level. Coincident with this suprahyperpolarization, the vasomotor response to hypoxia is fundamentally altered. Instead of the compensatory dilation observed in the normal retina, arterioles constrict in response to an oxygen deficiency. This anomalous vasoconstriction, which would potentiate hypoxia, raises the possibility that the bioelectric impact of neovascularization on vascular function is a previously unappreciated pathophysiological mechanism to sustain hypoxia-driven angiogenesis.

neovascularization | proliferative retinopathy | retinopathy of prematurity | proliferative diabetic retinopathy | retina

The abnormal growth of blood vessels is a key pathophysiological feature of numerous disorders, including tumorigenesis, arthritis, endometriosis, and retinopathies. Despite substantial progress from studies of patients and animal models, abnormal neovascularization remains a common threat to health and well-being. To help address this challenge, we devised a unique experimental approach to better understand neovascular pathophysiology. Because almost nothing is known about the electrogenic profile of neovascular complexes and how these complexes functionally interact with their parent vessels, we focused on the bioelectric features of neovascularization. These gaps in knowledge are surprising, considering that it is well established that the transmembrane voltage of vascular cells (1), as well as electrotonic cell–cell interactions within a vascular network (2–4), play vital roles in regulating blood flow.

In this electrophysiological analysis of pathological angiogenesis, we focused on abnormal vasoproliferation in rodent and human retinas. For multiple reasons, the retina is an ideal tissue for this undertaking. First is its clinical importance. Retinal vasoproliferation is the major cause of blindness in prematurely born infants (retinopathy of prematurity) and persons with diabetes (proliferative diabetic retinopathy) and sickle cell disease (sickle cell retinopathy). The hallmark of these disorders is abnormal growth of new blood vessels (neovessels) triggered by failure of the retinal vasculature to adequately supply oxygen and nutrients. Unfortunately, rather than improving the metabolic status, neovessels sprouting from the retinal vasculature extend aberrantly onto the surface of the retina, where they form preretinal neovascular complexes, which have a propensity to bleed and to detach the underlying retina, profoundly interfering with visual function.

A second reason for studying pathological angiogenesis in the retina is the availability of well-characterized rat and mouse models of retinal neovascularization (5–7). In the most commonly used rodent models, experimental alteration of the ambient oxygen level in early postnatal life disrupts retinal vascular development, resulting in the growth of neovessels onto the retinal surface, where blood vessels are never found under physiological conditions. The clinical relevance of these models is supported by the similarity of their preretinal neovascular complexes with those observed in infants with retinopathy of prematurity (ROP) (8). Of practical importance, the preretinal location of pathological neovascular complexes makes them relatively easy targets for electrophysiological recording.

A third experimental advantage is the ability to maintain rodent retinas ex vivo for many hours. Finally, the retina is an excellent tissue for beginning an exploration of the bioelectric impact of pathological angiogenesis because we can obtain electrophysiological recordings not only from rodent models, but also from human neovascular specimens excised during surgery for sight-threatening complications of proliferative diabetic retinopathy.

In this study, our perforated-patch recordings revealed that aberrant preretinal neovascular complexes generate extraordinarily high voltage. Owing to the bioelectric interactions between tufts of neovessels and the intraretinal parent vasculature, hyperpolarizing voltage is transmitted into the retinovascular network. When the number of neovascular complexes is abundant, this voltage input is substantial and boosts the membrane potential of

Significance

Angiogenesis is essential for the health of all vertebrates, but the outgrowth of new blood vessels also plays a role in disease by facilitating tumorigenesis, boosting inflammation, and causing blindness. Despite intensive investigation, pathological angiogenesis remains a formidable clinical challenge. Here we adopted an experimental strategy focusing on the bioelectric impact of neovascularization. Surprisingly, although the transmembrane voltage of vascular cells is known to regulate blood flow, no previous electrophysiological analysis of pathological angiogenesis has been reported. Using animal models and human specimens of retinal neovascularization, we discovered that neovascular complexes generate an extremely high voltage, whose transmission into the retinovascular network exerts a function-altering impact. Uncovering bioelectric mechanisms in the pathogenesis of neovascularization is likely to reveal new therapeutic targets.

Author contributions: D.G.P. designed research; D.G.P., R.K., Y.F., T.W.G., and D.A.P.-C. performed research; D.G.P., R.K., Y.F., and D.A.P.-C. analyzed data; and D.G.P. wrote the paper.

The authors declare no conflict of interest.

This article is a PNAS Direct Submission.

Freely available online through the PNAS open access option.

[1]To whom correspondence should be addressed. Email: dgpuro@umich.edu.

This article contains supporting information online at www.pnas.org/lookup/suppl/doi:10.1073/pnas.1604757113/-/DCSupplemental.

www.pnas.org/cgi/doi/10.1073/pnas.1604757113

retinal blood vessels to a suprahyperpolarized level. Associated with suprahyperpolarization, the vasomotor response to hypoxia is fundamentally altered. Instead of the compensatory vasodilation observed in normal retina, hypoxia triggers arterioles to constrict. Because this anomalous vasoconstriction would delimit oxygen delivery to the hypoxic sites of vasoproliferation, the bioelectric impact of pathological angiogenesis on vascular function may serve to sustain hypoxia-driven neovascularization.

Results

Vascular Suprahyperpolarization in Pathological Angiogenesis. In initial experiments using the rat ROP model of Penn and coworkers (5), we measured vascular voltages in ex vivo retinas of postnatal day (P) 17–P20 pups. At this age, there was robust vasoproliferation in the context of an experimentally-induced retardation of retinal vascularization (Fig. 1*A* and Fig. S1 *A* and *B*). Perforated-patch recordings revealed that pathological neovascular complexes aberrantly located on the retinal surface had an extraordinarily high mean resting membrane potential of −95 ± 8 mV (range, −83 to −110 mV; median, −94 mV; $n = 23$) (Fig. 1*B*).

In addition, we found that intraretinal blood vessels located beneath clusters of preretinal neovascular complexes were also extremely hyperpolarized in P17–P20 ROP retinas. Using pipettes sealed onto abluminal mural cells located on the outer walls of arterioles with diameters of 10–20 μm, we measured a mean membrane potential of −92 ± 6 mV (range, −75 to −103 mV; median, −92 mV; $n = 16$) (Fig. 1*C*). This suprahyperpolarization contrasts sharply with the mean membrane potential of −50 ± 6 mV (range, −41 to −60 mV; median, −51 mV; $n = 14$; $P < 0.0001$) recorded in arterioles located within ex vivo retinas of age-matched control rats (Fig. 1*D*).

To bolster the experimental support for suprahyperpolarization being a bioelectric feature of pathological retinal angiogenesis, we measured vascular voltages in another animal model, oxygen-induced retinopathy (OIR) in mice (6). In ex vivo retinas at P16–P18 (the period of abundant neovascularization in this model), the mean membrane potentials of preretinal neovascular complexes and intraretinal vessels were −87 ± 5 mV (range, −80 to −95 mV; median, −86 mV; $n = 9$) and −84 ± 8 mV (range, −68 to −92 mV; median, −83 mV; $n = 8$), respectively. In contrast, the mean resting membrane potential of blood vessels within age-matched ex vivo control mouse retinas was −62 ± 15 mV (range, −40 to −84 mV; median, −57 mV; $n = 13$; $P \leq 0.0012$).

Having found extremely high voltages in the two most commonly studied animal models of retinal neovascularization, we then asked whether suprahyperpolarization is also a feature of pathological retinal angiogenesis in humans. To address this question, we obtained perforated-patch recordings from blood vessels within preretinal complexes freshly excised from adult patients undergoing surgery for complications of proliferative diabetic retinopathy (Fig. 2). In these surgical specimens, the mean vascular voltage was −100 ± 7 mV (range, −89 to −108 mV; median, −101 mV; $n = 5$ recordings from 4 specimens). Although limited by the uncommon availability of appropriate surgical tissue, these recordings support the pathophysiological concept that suprahyperpolarization is a bioelectric characteristic of pathological retinal angiogenesis in humans and rodents. Furthermore, suprahyperpolarization is a feature of neovascular complexes in mature as well as developing retinas.

Impact of Neovascular Regression on Suprahyperpolarization. In additional experiments using the rat ROP model, we extended the age range studied to ascertain whether suprahyperpolarization persists as neovascular complexes regress spontaneously. Neovascular regression is common in human ROP and commences in the rat model during the fourth postnatal week when the peripheral retina becomes vascularized (Fig. S1 *A* and *B*). As shown in Fig. 1*B*, residual preretinal neovascular complexes remain suprahyperpolarized through at least P60 despite extensive neovascular regression (Fig. S1 *B* and *C*). In contrast to the persistent suprahyperpolarization of neovascular complexes, the membrane potential of blood vessels within ROP retinas decreases markedly after ∼P30 (Fig. 1*C*) to voltages similar to those of control retinas (Fig. 1*D*).

The observation that after P30, preretinal neovascular complexes remain suprahyperpolarized while the intraretinal vasculature depolarizes (Fig. 1 *B* and *C*) indicates that neovascular suprahyperpolarization is not dependent on voltage generated by intraretinal vessels. Additional strong evidence that neovascular suprahyperpolarization is not dependent on voltage derived from the retinovasculature is the previously noted finding that pathological neovascular complexes excised from the surface of human retinas exhibit an extremely high membrane potential of −100 mV. Thus, we conclude that suprahyperpolarization is an intrinsic bioelectric feature of pathological preretinal neovessels.

Neovascular-Driven Suprahyperpolarization. To guide further experimentation, we formulated a bioelectric model based on the working hypothesis that intrinsically suprahyperpolarized preretinal neovessels electrotonically transmit voltage to underlying parent intraretinal vessels. This model predicts that when neovascular

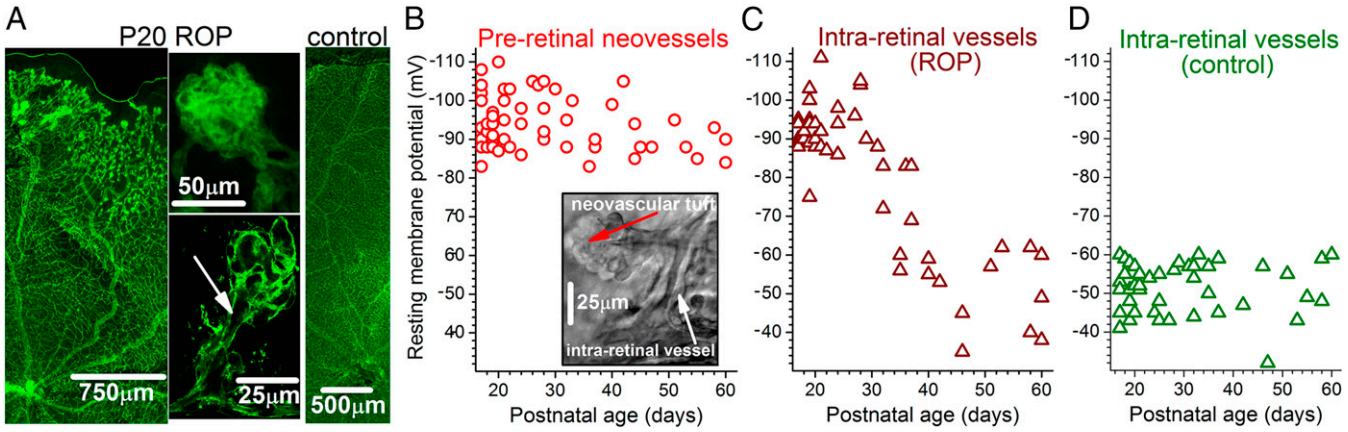

Fig. 1. Vascular voltages in ex vivo retinas of P17 to P60 ROP and control rats. (*A*) Ex vivo retinas stained with the endothelial marker isolectin GS-IB_4. (*Left*) A P20 ROP retina with preretinal neovascular complexes in the periphery. (*Center*) Preretinal neovascular complexes shown at higher magnification. The lower panel is a confocal image with an arrow showing the lumen linking the neovascular tuft with its parent vessel. (*Right*) Control rat retina. (*B*) Resting membrane potentials of preretinal neovascular complexes in rat ROP retinas. (*Inset*) Image of an ex vivo P19 ROP retina in which a perforated-patch pipette was sealed onto the preretinal neovascular tuft. (*C*) Voltages of arterioles located in the superficial vascular layer beneath preretinal neovascular complexes of ROP retinas. (*D*) Arteriolar voltages in the superficial vascular layer of control retinas.

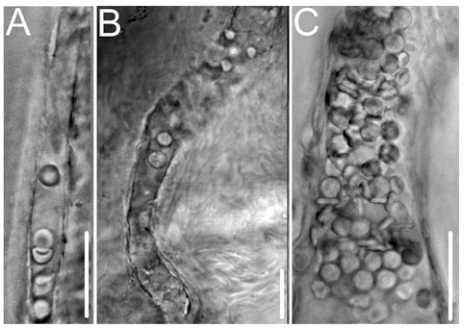

Fig. 2. Images of preretinal neovascular complexes excised from adult diabetic patients. Voltages were −104 mV in *A*, −89 mV in *B*, and −101 mV in *C*. Unlike the neovascular complexes of the rodent models, the surgical specimens had extensive fibrosis and had been in eyes that had received laser-induced retinal ablation and, in most cases, anti-vascular endothelial growth factor molecules. Despite these differences, suprahyperpolarization is a bioelectric feature of human, as well as rodent, retinal neovascularization. (Scale bars: 25 μm.)

complexes are relatively abundant, the input of neovessel-generated voltage can boost the retinovasculature's membrane potential to a suprahyperpolarized level. Conversely, when neovessels are sparse, their impact on the voltage of intraretinal vessels is minimal.

An essential feature of our interactive bioelectric model for pathological angiogenesis is that preretinal and intraretinal vessels are electrotonically coupled. To definitively demonstrate this coupling, we obtained simultaneous dual perforated-patch recordings from preretinal neovascular complexes and underlying parent vessels in ex vivo ROP retinas (Fig. 3*A*). In each of four successful dual recordings, the injection of a voltage-changing current via one of the recording pipettes resulted in a change in the membrane potential at the passively monitored site. In this series, electrotonic transmission was demonstrated in P17, P24, P42, and P53 ROP retinas; for these ages, the ratio of the voltage change detected at the responding site vs. the voltage change induced at the stimulated site was 0.15, 0.24, 0.40, and 0.15, respectively. Thus, preretinal and intraretinal vessels are electrotonically coupled. Furthermore, even though 98% of the neovascularization regressed by the sixth postnatal week (Fig. S1*B*), we detected electrotonic transmission between residual neovascular complexes and the retinovasculature.

In addition to dual recording experiments, data from single pipette recordings from ex vivo ROP retinas also lend support for a bioelectric model in which preretinal neovascular complexes drive the hyperpolarization of intraretinal vessels. As shown in Fig. 3*B*, the membrane potential of a sampled arteriole is correlated with the amount of pathological neovascularization in the locale (i.e., within 100 μm) of the recording site. When the total area of overlying neovascularization within a 100-μm radius is >10%, the underlying intraretinal vasculature is suprahyperpolarized; conversely, when the neovascular area regresses to <10%, as observed after ∼P30 (Fig. S1*B*), the voltage of intraretinal vessels drops. Taken together, data from dual and single recordings suggest that the decline in retinovascular voltage observed after P30 is not due to cessation of electrotonic transmission between preretinal and intraretinal vessels. Rather, it appears likely that retinovascular depolarization is a consequence of neovascular regression causing a decrease in the number of preretinal neovessels available to transmit hyperpolarizing voltage into the intraretinal vascular network.

Retinovascular Spread of Neovessel-Generated Voltage. Although this bioelectric analysis of pathological angiogenesis focused chiefly on preretinal neovascular complexes and the intraretinal vessels located beneath these complexes, a critical question is whether the hyperpolarizing neovascular input spreads more widely through the retinovasculature. Using P17–P22 ROP retinas, we addressed this question by recording arteriolar voltages at sites distant from where the sampled vessel passed below preretinal neovascular complexes. As shown in Fig. 3*C*, suprahyperpolarization extends well beyond the location of neovascularization. Based on these data, it appears that as neovessel-generated voltage spreads efficiently along an intraretinal arteriole with decay rate of only ∼5% per 100 μm, which is strikingly similar to the highly interactive electrotonic architecture of the retinovasculature in normal adult rats (4). Thus, the bioelectric impact of pathological neovascularization extends well beyond its physical location in the retina.

Electrogenic Basis for Neovessel Suprahyperpolarization. What electrogenic mechanisms account for neovascular suprahyperpolarization? To help address this question, we devised an experimental preparation consisting of microvessels (i.e., outer diameter <20 μm) freshly isolated from ROP retinas. Similar to the neovascular complexes in intact ROP retinas, isolated ROP vessels contain suprahyperpolarized (mean, −90 ± 15 mV; range, −60 to −118 mV; median, −92 mV; $n = 87$) complexes of endothelial cells (Fig. S2). This preparation was experimentally advantageous, because possible confounding effects mediated by nonvascular cells were eliminated, and also because the ability to obtain approximately three vessel-containing coverslips per retina allowed a marked reduction in the number of ROP rats required for electropharmacologic assays.

In a series of voltage-clamp experiments, perforated-patch pipettes were sealed onto the suprahyperpolarized complexes and inhibitors of various ion channels and electrogenic transporters/pumps were used to establish a bioelectric profile. For comparison, we also determined the electrogenic features of vessels isolated from control retinas. As summarized in Fig. 4, the major hyperpolarizing influences in the ROP complexes are (*i*) basally active ATP-sensitive potassium (K_{ATP}) channels, (*ii*) an extremely negative equilibrium potential for the electrogenic Na^+/Ca^{2+} exchangers (E_{NCX}), and (*iii*) a relatively small nonspecific cation (NSC) conductance. Supporting the validity of this bioelectric profile, a limited number of recordings from neovascular complexes located on the surface of ex vivo ROP retinas also detected a basal K_{ATP} conductance (1,350 ± 330 pS; $n = 3$), a markedly hyperpolarized E_{NCX} (−110 ± 15 mV; $n = 3$), and a low NSC conductance (270 ± 95 pS; $n = 3$).

Of note, with E_{NCX} being more negative than the equilibrium potential for K^+ ($E_K = -90$ mV), the outward current generated as NCX runs in its "reverse" mode (1 Ca^{2+} in, 3 Na^+ out) is

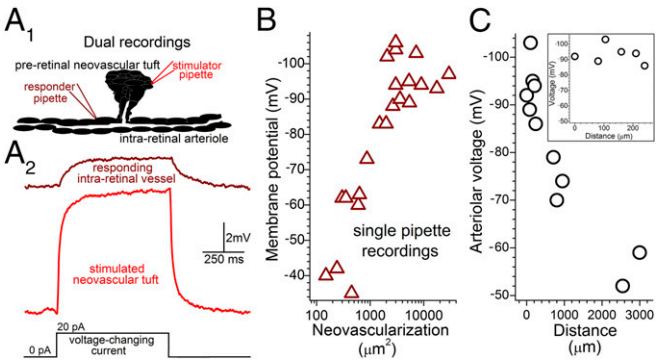

Fig. 3. Bioelectric interactions between preretinal neovascular complexes and intraretinal vessels in ex vivo ROP retinas. (*A*, *1*) Schematic of simultaneous dual perforated-patch recordings. (*A*, *2*) Voltage traces from a passively monitored intraretinal vessel (*Upper*) and a nearby preretinal neovascular complex (*Lower*), whose current-induced 8.4-mV depolarization caused a 2-mV voltage decrease at the passive site. (*B*) Intraretinal arteriolar voltages versus amount of preretinal neovascularization ≤100 μm from the recording site. (*C*) Voltages of intraretinal arterioles recorded in ex vivo P17–P22 ROP retinas at locations distant from preretinal neovascular complexes. 0-μm data are from Fig. 1*C*. (*Inset*) Enlarged distance scale showing the low decay rate of voltage spreading from sites of preretinal neovascularization.

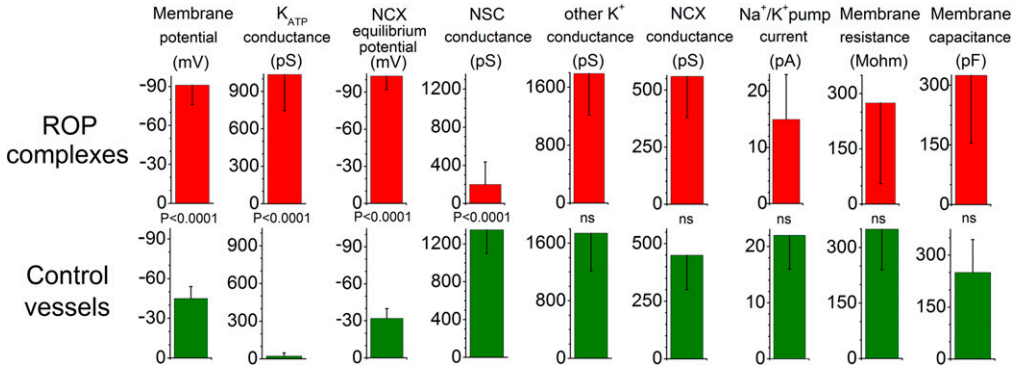

Fig. 4. Bioelectric profiles. (*A*) Electrogenic parameters of suprahyperpolarized vascular complexes on freshly isolated ROP vessels. *Lower panel*, electrogenic features of vessels from control rat retinas. Table S1 provides additional data.

capable of driving the membrane potential beyond E_K, which in fact was observed in 36 of 69 neovascular complexes sampled in ex vivo ROP retinas (Fig. 1*B*). Interestingly, although it is known that the reverse mode of NCX operation (rNCX) is critical for the angiogenic actions of vascular endothelial growth factor (9)—the target for existing medical treatments of vasoproliferative retinal disorders—there is no previous electrophysiological documentation of rNCX function in pathological angiogenesis.

How is the bioelectric profile of neovascular complexes established? Because preretinal neovascular tufts contain high levels of oxidants (10), we hypothesized that oxidation may play a role. To assess this possibility, we exposed isolated ROP vessels to the antioxidant n-acetyl cysteine (NAC; 100 μM). This treatment decreased the K_{ATP} conductance by 82 ± 12% ($n = 6$; $P < 0.0001$) (Table S1). This effect is consistent with the known redox sensitivity of retinovascular K_{ATP} channels, the activity of which in retinal vessels of normal rats is boosted by oxidants (11, 12). In contrast, this NAC treatment did not significantly affect E_{NCX} or the NSC conductance (Table S1). Nevertheless, an impact of oxidation on the function of these electrogenic components cannot be completely excluded; more experiments might reveal a statistical significance of the small differences shown in Table S1. In fact, vascular E_{NCX} appears to be somewhat oxidant-sensitive, with exposure of normal retinal microvessels to the oxidant, H_2O_2 (30 μM), modestly increasing the mean E_{NCX} value from −32 ± 8 mV ($n = 18$) to −40 ± 6 mV ($n = 6$; $P = 0.037$). On the other hand, our earlier observation that H_2O_2 activates NSC channels in retinal vessels (13) is contrary to a scenario in which endogenous neovascular oxidants inhibit the NSC conductance. Taken together, our data indicate that oxidation is likely to account for the basal activation of K_{ATP} channels in neovascular complexes, although the mechanisms playing the predominant roles in minimizing NSC conductance and establishing an extremely negative E_{NCX} remain uncertain and require future investigation.

Functional Impact of Suprahyperpolarization. In our interactive bioelectric model of pathological retinal angiogenesis, we hypothesized that the electrotonic transmission of voltage from suprahyperpolarized neovascular complexes exerts a function-altering impact on the intraretinal vasculature. Specifically, we postulated that vasomotor responses mediated by a K^+ channel-induced voltage change could be affected by suprahyperpolarization, because K^+ channel activation cannot induce a change in voltage when the membrane potential is near E_K, as is the case for <P30 ROP retinovessels (Fig. 1*C*). To assess this possibility, we monitored the vasomotor response to hypoxia, which triggers a compensatory vasodilation in normal retinas (14). The response to hypoxia was of interest because K_{ATP} channels are activated in hypoxic retinal vessels (12) and play a role in vasodilation (15). Of further relevance, pathological angiogenesis occurs in the context of retinal hypoxia.

In a series of experiments, we monitored lumens of intraretinal arterioles (8–15 μm inner diameters). In <P30 ROP retinas, the monitored vessels were in areas containing preretinal neovascular complexes. As summarized in Fig. 5, the vasomotor response to hypoxia was fundamentally different in <P30 ROP retinas compared with control retinas. Namely, instead of the compensatory vasodilation observed in control retinas, exposure of <P30 ROP retinas to a deoxygenated bathing solution triggered constriction of arterioles. Consistent with the importance of suprahyperpolarization, hypoxia resulted in the dilation of >P40 ROP retinovessels (Fig. 5), whose resting membrane potentials are no longer suprahyperpolarized (Fig. 1*C*). These findings suggest that neovascular-driven suprahyperpolarization compromises the ability of the retinovasculature to ameliorate an oxygen deficiency.

Hypoxia-Induced Vasoconstriction: Role of Lactate. What mechanism accounts for the vasoconstriction observed in hypoxic <P30 ROP retinas? We hypothesized that vasoactive molecules, such as adenosine, nitric oxide (NO), and lactate, which are released by hypoxic cells and have putative roles in angiogenesis (16–18), may play a role. As summarized in Fig. 5, neither adenosine nor the NO donor, sodium nitroprusside, mimicked the vasoconstrictive effect of hypoxia in ex vivo <P30 ROP retinas; instead, they caused arterioles to dilate. However, similar to hypoxia, exposure to lactate triggered arterioles in <P30 ROP retinas to constrict (Fig. 5). Also similar to hypoxia and consistent with lactate's role as a vasodilator in the normal retinas (15, 19–21), arterioles within both control and >P40 ROP retinas—whose vessels were not suprahyperpolarized (Fig. 1*C*)—dilated in response to lactate (Fig. 5).

Indicative that the vasomotor effects of lactate are dependent on its uptake via monocarboxylate transporters (MCTs), lactate did not elicit a detectable change in arteriolar lumens in retinas pretreated with the MCT inhibitor 2-cyano-3-(4-hydroxyphenyl)-2-propenoic acid (CHC) (22) (Fig. 5). Furthermore, CHC's prevention of hypoxia-induced vasoconstriction in <P30 ROP retinas (Fig. 5) indicates that this anomalous response is triggered by the uptake of endogenously produced lactate.

How does the uptake of lactate in <P30 ROP retinas result in vasoconstriction? Based on our earlier study of retinovessels (20), we considered a role for a cascade of events involving lactate, MCT, and NCX. Previously, we found that under certain conditions, the activation of this cascade can cause retinovessels to contract (20), although this vasoconstricting influence is usually vitiated by the potent vasorelaxing impact of lactate on precapillary arterioles (21), as well as on larger retinal arterioles, in which the activation of a voltage-changing K_{ATP} current plays a key role (15). However, we posited that the relative impact of the lactate/MCT/NCX pathway would be boosted when suprahyperpolarization to a voltage near E_K, as observed in <P30 ROP retinas (Fig. 1*C*), precludes a K^+ channel-induced change in voltage. Consistent with this scenario, we did not detect

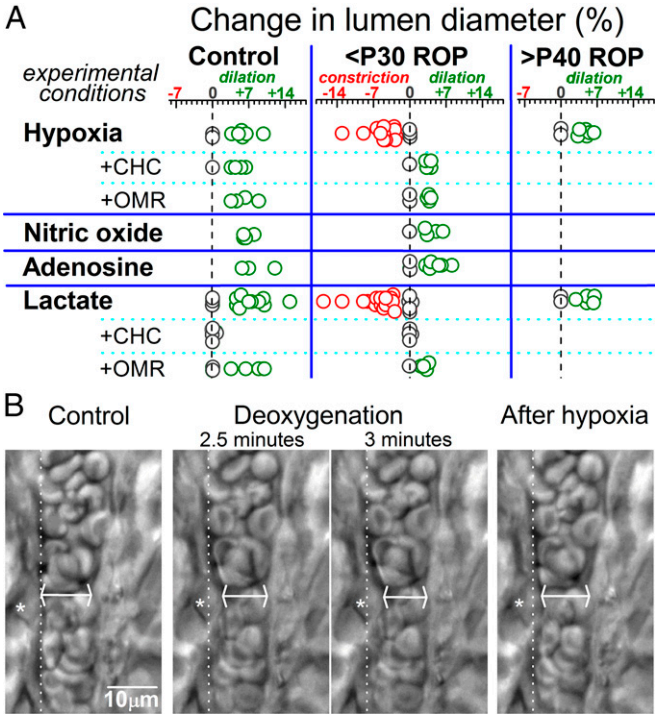

Fig. 5. Vasomotor responses in ex vivo retinas. (*A*) Arterioles with lumens of 8–15 μm were monitored during exposure to a deoxygenated perfusate (hypoxia), the NO donor sodium nitroprusside (100 μM), 5 μM adenosine, or 40 mM lactate. Responses to hypoxia and lactate were also tested in the presence of an inhibitor of monocarboxylate transporters, CHC (1 mM), and an NCX inhibitor, OMR-10103 (5 μM). (*B*) Images of an arteriole within an ex vivo P17 ROP retina before, during, and 5 min after exposure to a deoxygenated bathing solution. Asterisks denote a contracting abluminal cell, whose original position before hypoxia is shown by the dotted lines. At the site of maximal narrowing (arrows), the lumen decreased from 10.2 μm to 8.8 μm during hypoxia. In contrast to the compensatory vasodilation observed in control retina, the suprahyperpolarized vasculature of <P30 ROP retinas respond to hypoxia with an anomalous vasoconstriction.

vasoconstrictive responses to lactate or hypoxia in <P30 retinas that had been pretreated with the NCX inhibitor OMR-10103 (23) (Fig. 4). Taken together, our pharmacologic experiments point to roles for endogenously produced lactate, monocarboxylate transporters, and Na^+/Ca^{2+} exchangers in mediating the anomalous vasoconstrictive response to hypoxia observed in <P30 ROP retinas.

Discussion

This bioelectric analysis of pathological angiogenesis reveals that preretinal tufts of neovessels aberrantly sprouting from blood vessels within rodent and human retinas generate extraordinarily high resting membrane potentials. Electrophysiological recordings further demonstrated that neovessels and parent vessels interact bioelectrically. As a consequence of this electrotonic coupling, hyperpolarizing voltage is transmitted from neovascular complexes into the retinovascular network. When pathological neovascularization is extensive, the membrane potential of retinal vessels is boosted to a suprahyperpolarized level. We found that with this suprahyperpolarization, the vasomotor response to hypoxia is fundamentally altered, so that hypoxia triggers arteriolar constriction rather than the compensatory vasodilation observed in normal retinas. By delimiting the delivery of oxygen to hypoxic sites of abnormal vasoproliferation, this response of the vasculature to hypoxia may play a previous unappreciated role in the pathogenesis of neovascularization.

In this study, we used ex vivo rodent retinas to obtain electrophysiological recordings from vessels of an intact retina. A caveat is that the retinal vasculature was not internally perfused, because it is not currently feasible to obtain patch-clamp recordings from pressurized arterioles within ex vivo or in vivo retinas. Given that luminal pressurization is known to cause vascular depolarization (24, 25), it is likely that the membrane potentials measured in our study are higher than those in vivo. However, the difference in voltage is likely modest, because the small retinal arterioles (<20 μm outer diameter) sampled in our study have a reported internal pressure of ∼30 mm Hg in vivo (26), which causes a depolarization of only ∼10 mV as indicated in analysis of nonocular vessels (25).

Consistent with this modest effect of pressurization, the voltage of blood vessels recorded in nonperfused ex vivo control retinas (Fig. 1*C*) was <10 mV more negative than the vascular voltages measured at experimentally advantageous in vivo sites, such as the rat cremaster muscle (−42 mV) and the hamster cheek pouch (−46 mV) (27, 28). Thus, a lack of internal pressurization does not account for the suprahyperpolarized membrane potentials of ∼-90 mV that we recorded in arterioles of nonperfused ex vivo <P30 ROP retinas (Fig. 1*C*). Furthermore, because blood flow in preretinal neovascular complexes in vivo is sluggish (29), it is unlikely that the suprahyperpolarized membrane potentials recorded in neovascular complexes (Fig. 1*B*) is due to a lack of internal perfusion. Thus, although it would be ideal to obtain electrophysiological recordings from vessels in internally perfused ex vivo retinas or in retinas in vivo, the foregoing considerations support the pathophysiological concept that suprahyperpolarization is a bioelectric characteristic of pathological retinal angiogenesis.

Because no previous electrophysiological analyses of pathological angiogenesis have been reported, it remains to be established whether suprahyperpolarization is a bioelectric feature of neovascularization at nonretinal sites. Nonetheless, because the fundamental mechanisms for hypoxia-driven neovascularization almost certainly evolved to meet the needs of nonretinal tissues, we posit that this may be the case. With retinal neovascularization only recently impacting health owing to increased life expectancies of premature infants and patients with diabetes or sickle cell disease, there has been little time for evolutionary pressure to optimize neovascular mechanisms to meet the unique anatomic and physiological challenges of the retina (30). In nonretinal tissues, neovascularization is well adapted to enhance functional recovery; for example, in stark contrast to pathological retinal angiogenesis, vasoproliferation in hypoxic muscle is a highly effective adaptive response, even though the neovessels grow aberrantly and fail to replicate the pattern of the original vascular network (31). In tissues in which hypoxia-driven vasoproliferation is beneficial, we propose that a mechanism in which neovascular-induced suprahyperpolarization causes vessels to constrict in response to a local oxygen deficiency is likely to sustain the hypoxic microenvironment needed to drive adaptive neovascularization. Unfortunately, in the retina, sustained neovascularization is never beneficial and causes blindness. Our hope is that elucidation of the bioelectric impact of pathological angiogenesis on vascular function will provide new targets for therapeutic intervention in vasoproliferative disorders of the retina. It will also be important to analyze neovascularization in nonretinal tissues and tumors from a bioelectric perspective, because this new approach is likely to lead to novel strategies for therapeutic interventions at these sites.

Materials and Methods

Experimental protocols for rodent and human tissue were approved by the University of Michigan's Institutional Animal Care and Use Committee and Institutional Review Board. The University of Michigan's Institutional Review Board approved the study without the need for patient consent, based on the experimental use of excised tissue that normally would be discarded during an intraocular procedure. Detailed information on the materials and experimental procedures used in this study is provided in *SI Materials and Methods*.

Rodent Models of Proliferative Retinopathy. The 50/10 variable oxygen protocol of Penn and coworkers (5) was used to generate a pathological retinal neovascularization that closely resembles ROP in infants. In mice, the protocol of Smith et al. (6) was followed to create a model of OIR in which aberrant preretinal neovascularization is most abundant at ∼P17.

Experimental Preparations. Numerous experiments were performed using intact ex vivo retinas of ROP rats, OIR mice, and age-matched controls. Another experimental preparation consisted of preretinal neovascular tissue excised from adult patients with diabetes undergoing surgery for sight-threatening complications of proliferative retinopathy. A third preparation consisted of microvessels (i.e., <20-μm diameter) freshly isolated from the retinas of normal and ROP rats aged P30–P60 (30). The vessels isolated from ROP retinas often contained ∼15- to 25-μm-diameter multicellular complexes with a positivity for the endothelial cell marker isolectin GS-IB_4 (Fig. S2) and a suprahyperpolarization (mean, −90 ± 15 mV; range, −40 to −118 mV; median, −92 mV; n = 87) strikingly similar to the neovascular complexes observed in intact ROP retinas (Fig. 1*A* and Fig. S1*C*).

Electrophysiology. Voltages and currents were monitored via perforated-patch pipettes. Ex vivo retinas and surgical specimens were viewed using differential interference contrast (DIC)/infrared (IR) optics at 400× using a 40× water immersion objective. Isolated microvessels were viewed with phase-contrast optics at 400× . In recordings from ex vivo retinas, pipettes were sealed onto preretinal neovascular complexes and/or abluminal mural cells on intraretinal arterioles (10–20-μm diameter) located within the superficial vascular layer underneath clusters of preretinal neovascular complexes. In surgical specimens, recordings were obtained from erythrocyte-containing vessels (Fig. 2). In the case of retinal microvessels isolated from control rats, recording pipettes were sealed onto abluminal cells. For microvessels from ROP retinas, their suprahyperpolarized endothelial complexes (Fig. S2) were the recording targets.

Isolectin *Griffonia simplicifolia*-IB_4 Staining. Fixed specimens were incubated with 5.7 μg/mL Alexa Fluor 488-conjugated isolectin GS-IB_4 from *G. simplicifolia* (Molecular Probes and Life Technologies).

Quantification of Neovascularization. Quantification was performed in living retinas positioned in the recording chamber and viewed with DIC/IR optics at 400× with a 40× water immersion objective. Measurements were from the 200-μm-diameter retinal region (i.e., a high-power field), in which the area covered by preretinal neovascular complexes was maximal. NIS Elements software (Nikon) aided this quantification.

Vasomotor Responses. Images of arterioles (inner diameter, 8–15 μm; outer diameter, 10–20 μm) located in the superficial vascular layer of ex vivo retinas viewed with DIC/IR optics at 400× with a 40× water immersion objective were captured at ∼30-s intervals with a digital camera (Photometrics Cool Snap) using 50- to 90-ms exposures. In ROP retinas, monitored arterioles were in the locale of preretinal neovascular complexes. Offline, a software package (NIS Elements version 4.0) facilitated the lumen measurements used to calculate the change in mean diameter during exposure to experimental solutions. Of note, similar to in vivo observations (32), changes in lumen diameter of arterioles in ex vivo retinas were not uniform along a vessel; this study used the maximal change detected within the well-focused portion (∼25-μm long) of a monitored vessel.

Chemicals. All chemicals were obtained from Sigma-Aldrich unless noted otherwise.

Statistical Analyses. Values are presented as mean ± SD. Student's t test was used to evaluate probability.

ACKNOWLEDGMENTS. We thank B. Berkowitz for lending equipment and sharing information about the rat model, A. Barajas-Espinosa for sharing knowledge about the mouse model, A. Liepa for generating the rodent models, S. Lentz for assisting with confocal microscopy, D. Murrel for providing graphics expertise, and B. Hughes for reviewing drafts of the manuscript. This work was supported by National Institutes of Health Grants EY012507, EY20582, EY007003, and DK020572; the Alliance for Vision Research; and the A. Alfred Taubman Medical Research Institute.

1. Jackson WF (2000) Ion channels and vascular tone. *Hypertension* 35(1 Pt 2):173–178.
2. Segal SS, Neild TO (1996) Conducted depolarization in arteriole networks of the guinea pig small intestine: Effect of branching of signal dissipation. *J Physiol* 496(Pt 1): 229–244.
3. Peppiatt CM, Howarth C, Mobbs P, Attwell D (2006) Bidirectional control of CNS capillary diameter by pericytes. *Nature* 443(7112):700–704.
4. Zhang T, Wu DM, Xu GZ, Puro DG (2011) The electrotonic architecture of the retinal microvasculature: Modulation by angiotensin II. *J Physiol* 589(Pt 9):2383–2399.
5. Barnett JM, Yanni SE, Penn JS (2010) The development of the rat model of retinopathy of prematurity. *Doc Ophthalmol* 120(1):3–12.
6. Smith LE, et al. (1994) Oxygen-induced retinopathy in the mouse. *Invest Ophthalmol Vis Sci* 35(1):101–111.
7. Hartnett ME, Penn JS (2012) Mechanisms and management of retinopathy of prematurity. *N Engl J Med* 367:2515–2526.
8. Wallace DK, Kylstra JA, Greenman DB, Freedman SF (1998) Significance of isolated neovascular tufts ("popcorn") in retinopathy of prematurity. *J AAPOS* 2(1):52–56.
9. Andrikopoulos P, et al. (2011) Ca^{2+} influx through reverse-mode Na^+/Ca^{2+} exchange is critical for vascular endothelial growth factor-mediated extracellular signal-regulated kinase (ERK) 1/2 activation and angiogenic functions of human endothelial cells. *J Biol Chem* 286(44):37919–37931.
10. Okuno Y, Nakamura-Ishizu A, Otsu K, Suda T, Kubota Y (2012) Pathological neoangiogenesis depends on oxidative stress regulation by ATM. *Nat Med* 18(8):1208–1216.
11. Ishizaki E, Fukumoto M, Puro DG (2009) Functional K_{ATP} channels in the rat retinal microvasculature: Topographical distribution, redox regulation, spermine modulation and diabetic alteration. *J Physiol* 587(Pt 10):2233–2253.
12. Nakaizumi A, Puro DG (2011) Vulnerability of the retinal microvasculature to hypoxia: Role of polyamine-regulated K_{ATP} channels. *Invest Ophthalmol Vis Sci* 52(13):9345–9352.
13. Fukumoto M, et al. (2012) Vulnerability of the retinal microvasculature to oxidative stress: ion channel-dependent mechanisms. *Am J Physiol Cell Physiol* 302(9):C1413–C1420.
14. Petersen L, Bek T (2015) Diameter changes of retinal arterioles during acute hypoxia in vivo are modified by the inhibition of nitric oxide and prostaglandin synthesis. *Curr Eye Res* 40(7):737–743.
15. Hein TW, Xu W, Kuo L (2006) Dilation of retinal arterioles in response to lactate: Role of nitric oxide, guanylyl cyclase, and ATP-sensitive potassium channels. *Invest Ophthalmol Vis Sci* 47(2):693–699.
16. Lutty GA, McLeod DS (2003) Retinal vascular development and oxygen-induced retinopathy: A role for adenosine. *Prog Retin Eye Res* 22(1):95–111.
17. Brooks SE, et al. (2001) Reduced severity of oxygen-induced retinopathy in eNOS-deficient mice. *Invest Ophthalmol Vis Sci* 42(1):222–228.
18. Sonveaux P, et al. (2012) Targeting the lactate transporter MCT1 in endothelial cells inhibits lactate-induced HIF-1 activation and tumor angiogenesis. *PLoS One* 7(3):e33418.
19. Brazitikos PD, Pournaras CJ, Munoz JL, Tsacopoulos M (1993) Microinjection of L-lactate in the preretinal vitreous induces segmental vasodilation in the inner retina of miniature pigs. *Invest Ophthalmol Vis Sci* 34(5):1744–1752.
20. Yamanishi S, Katsumura K, Kobayashi T, Puro DG (2006) Extracellular lactate as a dynamic vasoactive signal in the rat retinal microvasculature. *Am J Physiol Heart Circ Physiol* 290(3):H925–H934.
21. Jensen PS, Pedersen SMM, Aalkjaer C, Bek T (2016) The vasodilating effects of insulin and lactate are increased in precapillary arterioles in the porcine retina *ex vivo*. *Acta Ophthalmol*, 10.1111/aos.13025.
22. Halestrap AP, Meredith D (2004) The SLC16 gene family-from monocarboxylate transporters (MCTs) to aromatic amino acid transporters and beyond. *Pflugers Arch* 447(5):619–628.
23. Jost N, et al. (2013) ORM-10103, a novel specific inhibitor of the Na^+/Ca^{2+} exchanger, decreases early and delayed afterdepolarizations in the canine heart. *Br J Pharmacol* 170(4):768–778.
24. Loutzenhiser R, Chilton L, Trottier G (1997) Membrane potential measurements in renal afferent and efferent arterioles: Actions of angiotensin II. *Am J Physiol* 273(2 Pt 2): F307–F314.
25. Knot HJ, Nelson MT (1998) Regulation of arterial diameter and wall $[Ca^{2+}]$ in cerebral arteries of rat by membrane potential and intravascular pressure. *J Physiol* 508(Pt 1):199–209.
26. Glucksberg MR, Dunn R (1993) Direct measurement of retinal microvascular pressures in the live, anesthetized cat. *Microvasc Res* 45(2):158–165.
27. Segal SS, Bény JL (1992) Intracellular recording and dye transfer in arterioles during blood flow control. *Am J Physiol* 263(1 Pt 2):H1–H7.
28. Stekiel WJ, Contney SJ, Rusch NJ (1993) Altered beta-receptor control of in situ membrane potential in hypertensive rats. *Hypertension* 21(6 Pt 2):1005–1009.
29. Gass JD (1997) Macular dysfunction caused by retinal vascular disease. *Stereoscopic Atlas of Macular Diseases* (Mosby, St. Louis), 4th Ed, pp 437–599.
30. Puro DG (2012) Retinovascular physiology and pathophysiology: New experimental approach/new insights. *Prog Retin Eye Res* 31(3):258–270.
31. Dor Y, et al. (2002) Conditional switching of VEGF provides new insights into adult neovascularization and pro-angiogenic therapy. *EMBO J* 21(8):1939–1947.
32. Kornfield TE, Newman EA (2014) Regulation of blood flow in the retinal trilaminar vascular network. *J Neurosci* 34(34):11504–11513.
33. Schmidt TM, Kofuji P (2011) An isolated retinal preparation to record light response from genetically labeled retinal ganglion cells. *J Vis Exp* (47):e2367.
34. Berkowitz BA, Bansal N, Wilson CA (1994) Non-invasive measurement of steady-state vitreous lactate concentration. *NMR Biomed* 7(6):263–268.
35. Mishra A, et al. (2014) Imaging pericytes and capillary diameter in brain slices and isolated retinae. *Nat Protoc* 9(2):323–336.
36. Matsushita K, Puro DG (2006) Topographical heterogeneity of K_{IR} currents in pericyte-containing microvessels of the rat retina: Effect of diabetes. *J Physiol* 573(Pt 2):483–495.